ELSEVIER

Materials Science and Engineering B 120 (2005) 32–36

MATERIALS SCIENCE & ENGINEERING B

www.elsevier.com/locate/mseb

Domain structure studies on $Pb(Zn_{1/3}Nb_{2/3})O_3$–$PbTiO_3$ mixed crystal system

S. Madeswaran [a], S.V. Rajasekaran [a], R. Jayavel [a,*], S. Ganesamoorthy [b], G. Behr [c]

[a] *Crystal Growth Centre, Anna University, Chennai-25, India*
[b] *Laser Materials Division, Centre for Advanced Technology, Indore, India*
[c] *Leibniz Institute for Solid State and Materials Research, Dresden, Germany*

Abstract

In this investigation, ferroelectric $Pb(Zn_{1/3}Nb_{2/3})O_3$–$PbTiO_3$ single crystals have been grown by modified flux technique with PbO self flux. Well-defined domain patterns were observed through polarized light on the as-grown crystals. Fingerprint like pattern and tweed pattern have also been observed. In PZN–PT system the fingerprint domain area is found to be elongated along one direction for increasing PT content.

Keywords: PZN–PT single crystals; Ferroelectric domains; AFM

1. Introduction

Relaxor based single crystals, such as $Pb(B_{1/3}Nb_{2/3})O_3$–$PbTiO_3$ (B = Zn, PZN–PT; B = Mg, PMN–PT), have attracted much attention recently owing to their giant piezoelectric coefficient [1–4]. When these crystals are poled along its parent cubic ⟨0 0 1⟩ direction, piezoelectric coefficient d_{33} is enhanced to 2500 pC/N, electromechanical coupling factor k_{33} increases to 90% and piezoelectric strain of 1.5% has been obtained [4,5]. The domain structure and piezoelectric properties of ferroelectric single crystals of solid solution $Pb(Zn_{1/3}Nb_{2/3})O_3$–$PbTiO_3$ (PZN–PT) have a morphotropic phase boundary (MPB), which has been intensively investigated during the last decade [2,3,6,7]. The abnormal feature of this system is the extremely high piezoelectric effect in ⟨0 0 1⟩, while the spontaneous polarization direction being ⟨1 1 1⟩. This is attributed to the rotation of polarization from [1 1 1] to [0 0 1] by the phase transformation from rhombohedral to tetragonal phase. Such an ultrahigh piezoelectric effect has made these crystals as leading candidate for application in transducers, sensors and actuators especially in the field of medical ultrasonic imaging and underwater communication [4,5]. Since the piezoelectric properties of these crystals are fundamentally controlled by the ferroelectric domains, studies on domain structure and domain engineering in these materials are essential to achieve the desired properties. It has been shown that the relaxation phenomena in PMN crystals can be controlled by domain dynamics [8]. Several studies have been done on the domain structure of PZN–PT crystals, which revealed the existence of striped patterns and fingerprint patterns of nonferroelastic domains [9–12]. Piezoresponse force microscopy (PFM) is a modification of atomic force microscopy (AFM) based on converse piezoresponse effect and the ability of the conducting tip, to follow the piezoelectric vibration of the surface, which is locally excited by the ac voltage applied between the tip and the counter electrode. Recently, this technique has been shown to be a powerful tool for the visualization of domain structure at the submicron level even to the nanometer scale and has been applied to PZN–PT and PMN–PT crystals [6,10,13]. In this investigation, the preparation of PZN–PT single crystals and the domain structures observed on the grown crystals have been studied.

2. Experiment

$(1-x)Pb(Zn_{1/3}Nb_{2/3})O_3$–$xPbTiO_3$ ($x = 0.05$, 0.07 and 0.09) single crystals were grown by high temperature so-

* Corresponding author. Tel.: +91 44 22203571; fax: +91 44 22352870.
E-mail address: rjvel@annauniv.edu (R. Jayavel).

0921-5107/$ – see front matter © 2005 Elsevier B.V. All rights reserved.
doi:10.1016/j.mseb.2005.02.017

lution growth (flux) technique with PbO as flux [14]. The starting materials were weighed according to the stoichiometric proportion and then mixed with PbO flux and loaded into a 70 cm^3 platinum crucible. The crucible was sealed and buried into alumina powder in an alumina crucible and then sealed with alumina lid using alumina cement to prevent PbO evaporation. A oxygen cooling system was designed and assembled at the bottom of the crucible to have a large temperature gradient in order to induce single nucleation. The furnace temperature was controlled to 1170 °C using a proportional integral differential (PID) controller. The raw materials were soaked for 8 h and then oxygen flow was started. The furnace was slow cooled at a rate of 1–2 °C/h up to 900 °C and fast cooled to room temperature at a rate of 70 °C/h. Such a fast cooling rate is necessary to avoid pyrochlore phase. The bottom cooling arrangement is effective in inducing the concentrated nucleation at one point and enlarges the size of PZN–PT crystals by providing a large temperature gradient. After the growth, the crystals were harvested by boiling in 30% HNO_3 or acetic acid for more than 24 h. The grown crystals were oriented by X-ray Laue pattern and (0 0 1) and (1 1 1) slices were cut and polished for domain observation. Domain patterns were observed using optical polarized microscope and atomic force microscope. A commercial AFM (Seiko Instruments SPA 300, Japan) was used for the measurements. The scanned head allowed a maximum scan area of 150 μm. Surface structures on polished crystals were observed using AFM by contact topography and piezoresponse modes with an applied bias voltage of 18 V.

3. Results and discussion

Single crystals of PZN–7%PT grown by bottom cooling technique are shown Fig. 1. Fig. 1(a) and (b) show the as-grown crystals and cut and polished crystals, respectively. In the as-grown crystal, the nucleation starts at the crucible bottom and tends to grow up to the solution surface. They generally possess either irregular or arrow headed morphology. In many crystals the fast growing quadrant is perceptibly larger and assumed to have an arrowhead shape. Fang et al. [15] explained the crystallization procedure based on growth unit model, in which the crystal structure is composed of negative ion coordination polyhedrons whose couplings are positive ions. The coordination polyhedron possessing crystal structure is called a growth unit. From the kinetics viewpoint of crystal growth it is assumed that the growth mechanism mainly reveals the formation of growth units and the incorporation of growth units into the crystal lattice at the interface. PZNT is ionic crystal; the bonds of A–O and B–O in this structure are all ionic. In PZNT crystal, when [BO_6] octahedron is incorporated into (0 0 1) interface, it just bonds with one growth unit of (0 0 1) face with one terminal vertex. The stability of this assembling mode is poor. Therefore, only the formation of two-dimensional crystal nucleation can induce the growth at crystal corners or edges. When [BO_6] octahedron assembles into kinked (1 1 1) interface, it could bond with three vertexes of growth units using three terminal vertexes. When octahedrons assemble in this mode, the number of formation of chemical bond is more. Therefore, the terminal vertexes of the coordination octahedron have the strongest bonding force in this direction. Crystal growth along this direction does not follow the process of nucleation, and the growth rate is fast. Similarly, when [BO_6] octahedral growth unit is incorporated into (1 1 0) interface, the stability of this assembling mode will be in between the above two assembling modes. Hence the assembling of coordination octahedrons at different interfaces is different, and the growth rate of various crystal faces is related to the assembling modes of the growth units into different interfaces. Assembling of [BO_6] octahedral growth units into (1 1 1) interface has the strongest bonding force, and the direction of this crystal face has the fastest growth rate; the assembling of [BO_6] into (0 0 1) interface has the smallest bonding force, and this crystal face has the smallest growth rate resulting the arrowhead shape.

The domain structure in un-poled PZN–7%PT single crystal was visualized by the polarized optical microscope. The image in Fig. 2(a) exhibits pronounced bright and dark contrast with narrow strip-shaped or fingerprint domain patterns [16]. The domain patterns can be interpreted as ferroelectric domains with anti-parallel polarizations. It is noted that the domain regions are not uniform but combination of small domain regions with opposite contrasts, which are similar to those reported earlier [17]. Fig. 2(b) shows 90° domains observed through optical microscope for PZN–9%PT crystals. This complex domain observation confirms that domain structure of the morphotropic PZN–9%PT crystals, which is composed of both the rhombohedral and tetragonal (or monoclinic) orientation states.

Fig. 3(a) and (b) show typical topography and piezoresponse images of (0 0 1)-oriented PZN–5%PT single crystal. In both modes the contrast is so strong and the patterns seem to be island like complex structure. In the island like fingerprint pattern, the ferroelectric 180° domain walls have arbitrary orientation. It is seen in the *c*-domain of figure that there are two regions with bright and dark contrast corresponds to upper and lower height level, respectively. It is possible to identify the direction of spontaneous polarisation in the *c*-domain using electrostatic force microscope by measuring the surface potential due to the charge of the pyroelectric polarisation on the (0 0 1) plane [6]. It has been observed that the bright region corresponds to the tail of the polarisation and the dark region corresponds to the head of the polarisation. It is in agreement with the result obtained by other methods with low resolution [18].

The domain structures observed on PZN–7%PT and PZN–9%PT single crystals are shown in Fig. 4(a) and (b), respectively. In the topographic image of (0 0 1)-oriented PZN–9%PT single crystal, it is seen that the finger print (FP) domains and tweed pattern (TP) domains coexist in the same micron-size domain and a series of gradual transformation regions are clearly "frozen" as shown in Fig. 5(a). It is rea-

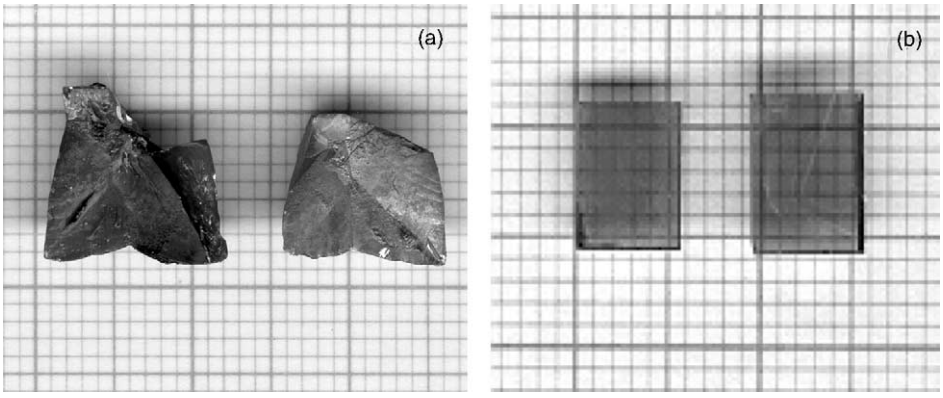

Fig. 1. (a) As-grown crystals of PZN–PT and (b) cut and polished wafers along (1 0 0) orientation.

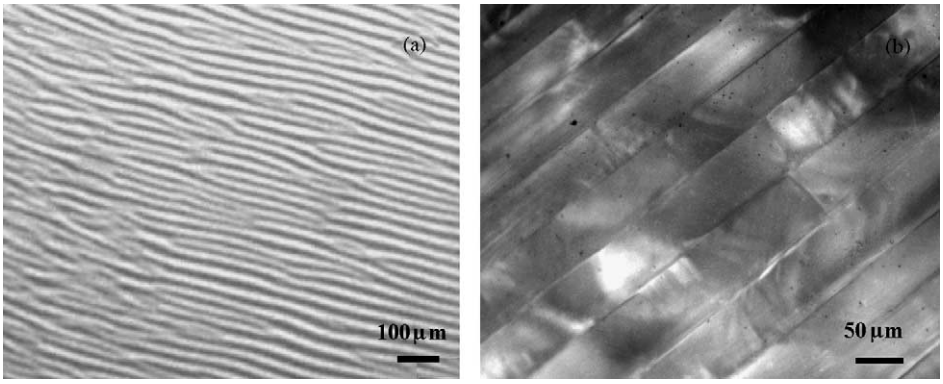

Fig. 2. (a) 180° finger print pattern and (b) 90° domains observed on PZN–9%PT crystal. This complex domain observation confirms that the domain structure of the morphotropic PZN–9%PT crystals is composed of both rhombohedral and tetragonal (or monoclinic) orientation states.

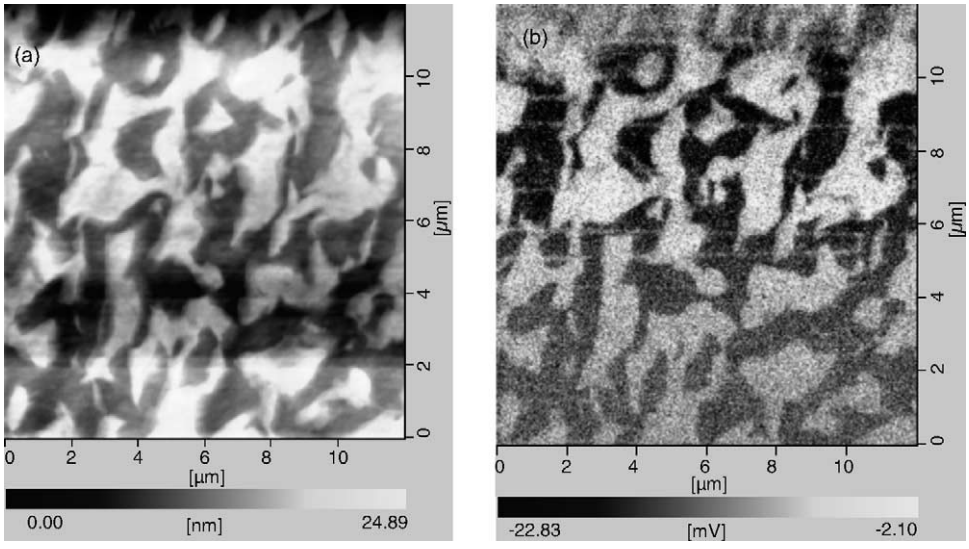

Fig. 3. (a and b) *c*–*c*-domains observed on PZN–5%PT crystal by atomic force microscopy using topography and piezoresponse mode, respectively. The dark and bright regions appear due to the positive and negative end of the dipoles.

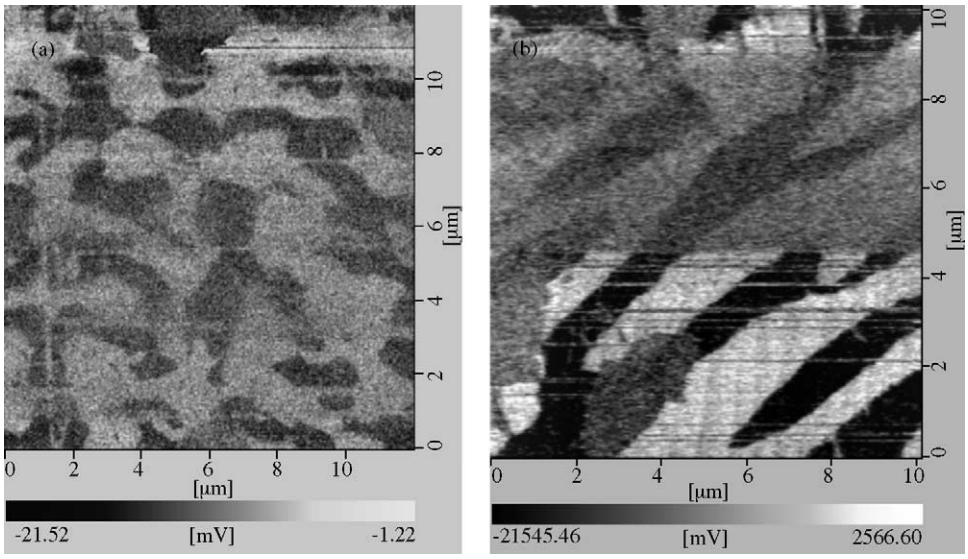

Fig. 4. Domains patterns observed on (a) PZN–7%PT and (b) PZN–9%PT single crystals by atomic force microscopy. Anti parallel *c*-domains make this bright and dark contrast. The 180° domains are elongated along [0 0 1] direction.

sonable to anticipate the FP domains and TP domains are intrinsically related. In Fig. 5(b), which was magnified from a part of the region scanned in Fig. 5(a), it is clearly seen that large micron-sized domains are not uniform and actually consist of small FP domains and TP domains with dimensions around 1–2 μm and ∼0.5 μm, respectively. It probably corresponds to the co-existence of rhombohedral and tetragonal phases in the PZN–9%PT single crystal. The FP domains or 180° antiparallel domains are ferroelectric and not ferroelastic because no strain is involved during domain formation or switching. On the other hand, the TP domains are not only due to ferroelectric, but also due to ferroelastic nature. These domains can be switched or reoriented by an applied stress and strain during domain formation, switching or reorientation. 180° and 90° domain walls are displayed in Fig. 5(b). The 180° domain walls reduce the depolarization energy, and the 90° domain walls reduce the strain energy produced during the phase transformation. The interaction between nano-polar clusters, which changes the short-range ordering into the long-range ordering promotes the reorientation and mergence of nano-clusters into irregular fingerprint pattern domain, as shown in Fig. 4(b). In this manner, the elastic strain energy of the ferroelectric transformation was stored in atomic-level [19]. The other tweed pattern domains begin to nucleate and grow in the FP domain to increase domain wall density and make the domain structure more complicated and irregular. It is well known that 180° domain walls have arbitrary orientation, while 90° domain walls have perfect orientation ⟨1 0 0⟩ or/and ⟨1 1 0⟩ in single crystal [17]. From all these observation (Figs. 3b, 4a and b) it is clear that

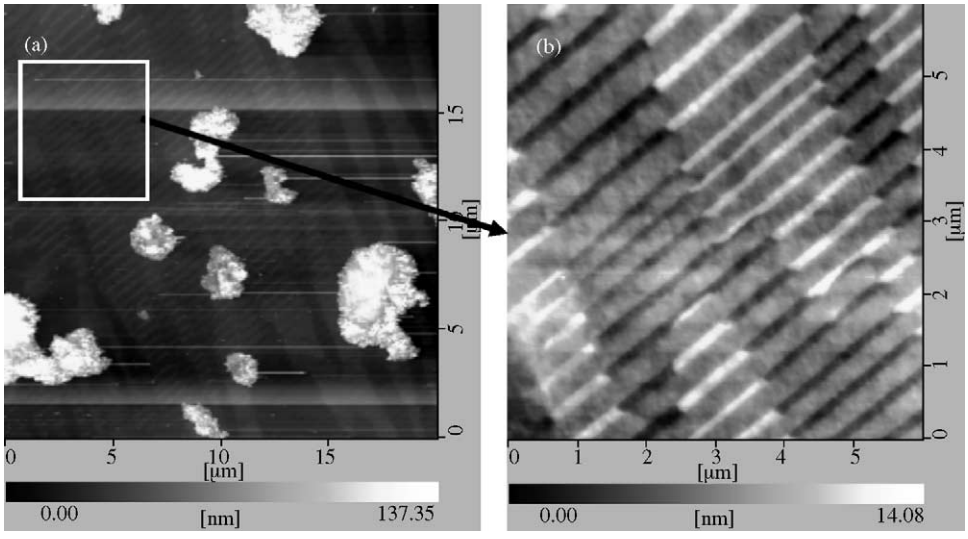

Fig. 5. (a) Tweed pattern domains observed on PZN–9%PT and (b) enlarged image. The 90° parallel domains are embedded in 180° domains structure.

the domain wall area is longer for higher PT, i.e. PZN–9%PT and elongated along only one direction. The complex domain structure in PZN–PT is attributed to some aberrations in the crystal lattice or chaotical distribution of defects in the crystals [17].

4. Conclusions

Piezoelectric single crystals of PZN–PT have been grown by bottom cooled flux technique. Fingerprint domains and parallel domain patterns have been observed on the grown crystals. It has been observed that small parallel domains with typical sizes of less than 0.5 μm are embedded in large size fingerprint pattern domains of ∼2–4 μm in (0 0 1)-oriented PZN–9%PT single crystals. Tweed patterns present in PZN–9%PT are not observed in crystals of low PT content (PZN–5%PT and PZN–7%PT). The fingerprint domains area increases and elongated in one direction for increasing PT content. The tweed pattern domains emerge in the fingerprint pattern increase the ferroelastic domain wall density in order to release the stress.

Acknowledgements

One of the authors, (SM) is grateful to the Council of Scientific and Industrial Research (CSIR), Government of India for the support under Senior Research Fellowship and thankful to Leibniz Institute for Solid State and Materials Research (IFW), Dresden for the support under DAAD programme. The authors are thankful to Dr. K. Kitamura and Dr. K. Terabe, Advanced Materials Laboratory, National Institute for Materials Science, 1-1 Namiki, Tsukuba, Japan for AFM observation.

References

[1] J. Kuwata, K. Uchino, S. Nomura, Jpn. J. Appl. Phys. 21 (1982) 1298.
[2] D. Damjanovic, Ann. Chim. Sci. Mater. 26 (2001) 99.
[3] S. Park, T.R. Shrout, IEEE Trans. Ultrason. Ferroelectr. Freq. Control 44 (1997) 1140.
[4] S. Saitoh, T. Takeuchi, T. Kobayashi, K. Harada, S. Shimanuki, Y. Yamashita, IEEE Trans. Ultrason. Ferroelectr. Freq. Control 46 (1999) 276.
[5] J. Yin, B. Jiang, W. Cao, IEEE Trans. Ultrason. Ferroelectr. Freq. Control 47 (2000) 285.
[6] M. Iwata, K. Katsuraya, I. Suzuki, M. Maeda, N. Yasuda, Y. Ishibashi, Jpn. J. Appl. Phys. 42 (2003) 6201.
[7] T. Yamamoto, K. Kawano, M. Saiti, S. Omika, Jpn. J. Appl. Phys. 36 (1997) 6145.
[8] A.E. Glazounov, A.K. Tagantsev, A. Bell, J. Phys. Rev. B 53 (1996) 11281.
[9] S. Shimanuki, S. Saito, Y. Yamashita, Jpn. J. Appl. Phys. 37 (1998) 3382.
[10] H.R. Zeng, Q.R. Yin, G.R. Li, H.S. Luo, Z.K. Xu, J. Crystal Growth 254 (2003) 432.
[11] I.K. Bdikin, V.V. Shvartsman, A.L. Kholkin, Appl. Phys. Lett. 83 (2003) 4232.
[12] H. Okino, J. Sakamoto, T. Yamamoto, Jpn. J. Appl. Phys. 142 (2003) 6209.
[13] M.C. Shin, S.J. Chung, S.G. Lee, R.S. Feigelson, J. Crystal Growth 263 (2004) 412.
[14] W. Tolksdorf, in: D.T.J. Hurle (Ed.), Handbook of Crystal Growth-Bulk Crystal Growth, Elsevier Science, North-Holland, Amsterdam, 1994.
[15] B.J. Fang, H.O. Xu, T.H. He, H.S. Luo, Z.W. Yin, J. Crystal Growth 244 (2002) 318.
[16] H. Schmid, in: N. Setter, E.L. Colla (Eds.), Ferroelectric Ceramics, Birkhauser Verlag, Basel, 1993, p. 07.
[17] M. Abplanalp, D. Barosova, P. Bridenbaugh, J. Erhart, J. Fousek, P.G. Unter, J. Nosek, M. Sulc, Solid State Commun. 119 (2001) 7.
[18] J. Liao, X.P. Jiang, G.S. Xu, H.S. Luo, Q.R. Yin, Mater. Charact. 44 (2000) 453.
[19] D. Viehland, J. Appl. Phys. 88 (2000) 4794.